

High-angular momentum excitations in collinear antiferromagnet FePS₃

Jan Wyzula,^{1,2} Ivan Mohelský,¹ Diana Václavková,¹ Piotr Kapuscinski,¹ Martin Veis,³
Clément Faugeras,¹ Marek Potemski,^{1,4} Mike E. Zhitomirsky,⁵ and Milan Orlita^{1,3}

¹Laboratoire National des Champs Magnétiques Intenses, EMFL,

CNRS UPR3228, Univ. Grenoble Alpes, Univ. Toulouse,

Univ. Toulouse 3, INSA-T, Grenoble and Toulouse, F-38042, France

²Department of Physics, University of Fribourg, Chemin du Musée 3, CH-1700 Fribourg, Switzerland

³Institute of Physics, Charles University, Ke Karlovu 5, Prague, CZ-121 16, Czech Republic

⁴CENTERA Labs, Institute of High Pressure Physics, PAS, PL-01-142 Warsaw, Poland

⁵Univ. Grenoble Alpes, CEA, IRIG, PHELIQS,
17 avenue des Martyrs, F-38000 Grenoble, France

We report on magneto-optical studies of the quasi-two-dimensional van der Waals antiferromagnet FePS₃. Our measurements reveal an excitation that closely resembles the antiferromagnetic resonance mode typical of easy-axis antiferromagnets, nevertheless, it displays an unusual, four-times larger Zeeman splitting in an applied magnetic field. We identify this excitation with an $|S_z| = 4$ multipolar magnon – a single-ion 4-magnon bound state – that corresponds to a full reversal of a single magnetic moment of the Fe²⁺ ion. We argue that condensation of multipolar magnons in large-spin materials with a strong magnetic anisotropy can produce new exotic states.

Magnons or quantized spin waves are collective excitations of localized magnetic moments in crystalline solids. These boson-like quasiparticles disperse with a lattice momentum \mathbf{k} , carry a fixed amount of energy and have an integer spin or angular momentum $S_z = \pm 1$. Magnons are optically active excitations, though due to vanishing momentum of photons, only spatially uniform spin waves are excited ($k = 0$ magnons). Despite the strictly quantum nature of magnons, their optical and magneto-optical response can be approached at the semi-classical level [1, 2], as transverse precession of coupled magnetic dipoles. In antiferromagnets, the related resonant absorption of light is referred to as the antiferromagnetic resonance (AFMR).

The AFMR has a particularly simple form in an antiferromagnet with a uniaxial anisotropy. Once an external magnetic field B is applied along the easy axis, the single AFMR mode splits into two frequency branches that are linear in B [2, 4]:

$$\omega_{\text{AF}} = \omega_{\text{AF}}^0 \pm \gamma B, \quad (1)$$

where γ stands for the gyromagnetic ratio. This implies the separation of branches equal to twice the Larmor frequency, or equivalently, to twice the Zeeman energy, $2E_Z = 2g\mu_B B$, with the g factor typically close to the free-electron value ($g = 2$).

The AFMR that follows such a simple rule was observed in the GHz/THz frequency range for many easy-axis antiferromagnets: in iron and manganese dihalides [5, 6] or in magnetic oxides [7–10], to name a few. At present, the AFMR in easy-axis antiferromagnets represents perhaps the most characteristic and easy-to-identify resonance/excitation in magnetic systems and it serves as a direct probe of the exchange coupling between spins and of the single-ion magnetic anisotropy.

In this Letter, we report on THz/infrared magneto-spectroscopy studies of the quasi-two-dimensional honeycomb antiferromagnet FePS₃, see Figure 1, which be-

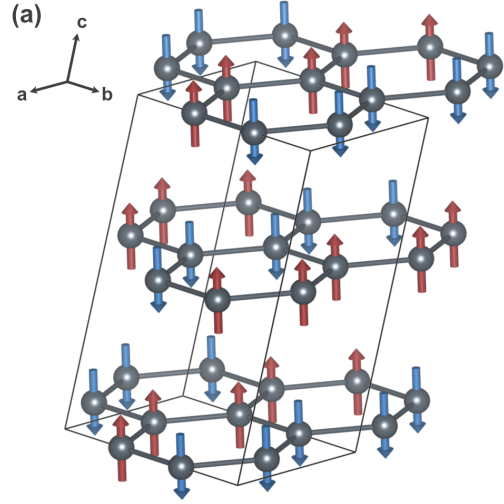


FIG. 1. The crystal lattice of FePS₃. The magnetic moments are color-coded to differentiate between the two orientations. The figure was created using the VESTA software [3].

longs to a topical family of magnetic van der Waals materials [12]. We find that the response is dominated by three types of magnetic excitations. Two of them correspond to conventional 1-magnon gaps which may, when the magnetic field is applied, be taken as text-book examples of the AFMR in easy-axis antiferromagnets. At the qualitative level, the third mode also resembles the AFMR, nevertheless, it displays four-times larger splitting of the branches. We show that this excitation corresponds to a full reversal of a single spin $S = 2$, which carries a total angular momentum of $|S_z| = 4$. Our observation extends the concept of single-ion bound states, so far limited to 2-magnon single-ion bound states in $S = 1$ systems [13], towards more complex excitations with a multipolar symmetry. In particular, for $S = 2$ magnetic

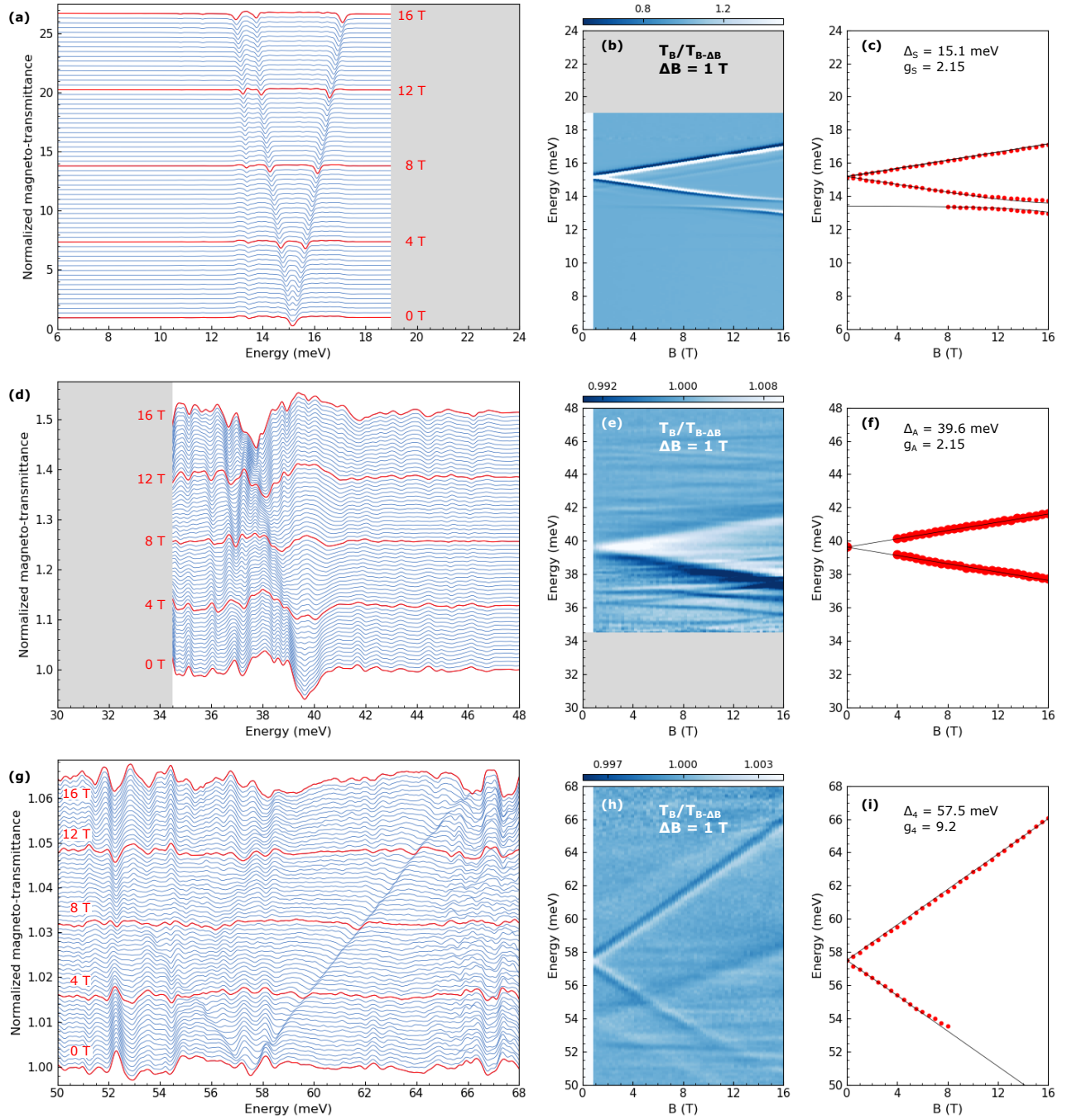


FIG. 2. Magneto-transmission of FePS₃ at $T = 4.2$ K in three spectral ranges showing the AFMR due to the lower 1-magnon gap Δ_S (a-c), the upper 1-magnon gap Δ_S (d-f) and the 4-magnon mode Δ_4 (g-i). The magneto-transmission spectra in (a), (d) and (g) were normalized by the averaged transmission T_B average over the explored interval $B = 0 - 16$ T. In panels (b), (e) and (h), differential magneto-transmission is plotted, $T_B/T_{B-\Delta B}$ for $\Delta B = 1$ T and the step in B of 0.25 T. The extracted position of all magnon branches (red circles) at selected B is presented in panels (c), (f) and (i) along with the theoretical fit (black lines). In panel (c), the theoretical fit uses the model and parameters described in Ref. 11. In panels (f) and (i), the fit assumes two linear-in- B AFMR-like branches. In gray areas, the explored FePS₃ sample was opaque.

materials, their condensation in a magnetic field may allow for exotic hexadecapole phases. Overall, our findings illustrate an emergence of exotic quantum excitations in semiclassical magnetic materials with large spins.

The infrared magneto-transmission experiments were carried out on a macroscopic FePS₃ bulk sample (with a surface area of 10 mm²) which was kept in helium exchange gas at temperature of 4.2 K and placed in a su-

perconducting solenoid. The magnetic field was always applied normal to the quasi-two-dimensional planes of FePS₃ and aligned with the wave vector of the probing radiation (Faraday configuration). To measure magneto-transmission, the radiation from globar was analyzed by a Bruker Vertex 80v Fourier-transform spectrometer, delivered to the sample via light-pipe optics and detected by a composite bolometer placed directly behind the sample. All presented data were collected using the spectral resolution of 0.125 meV.

The collected magneto-transmission data are presented in Figure 2 in three relevant spectral windows. To allow for a detailed inspection of these data, they are plotted in the form of magneto-transmission T_B , normalized by the transmission averaged over the whole range of B explored, in panels (a), (d) and (g), and also as false-color plots of differential magneto-transmission, $T_B/T_{B-\Delta B}$, in panels (b), (e) and (h). In each chosen window, the response is dominated by a single magnetic mode that splits into two linear-in- B branches, thus resembling closely the AFMR. These modes, denoted as M_S , M_A and M_4 , are centered at the photon energies of $\Delta_S = 15.1$ meV, $\Delta_A = 39.6$ meV and $\Delta_4 = 57.5$ meV, respectively. The deduced positions of both AFMR branches are plotted in parts (c), (f) and (i), respectively, as a function of B . The M_4 mode has the integral intensity roughly by a factor of 10^3 smaller as compared to M_S and M_A modes. Our data comprise even weaker spectral features, for instance, the AFRM-like modes at ~ 54 and 61 meV visible in Figure 2h, which are analyzed and discussed in the Supplementary materials [14].

The quasi two-dimensional antiferromagnet FePS₃ consists of honeycomb planes formed by Fe²⁺ ions with $S = 2$, see Figure 1. Below $T_N \approx 120$ K, FePS₃ orders in a collinear zig-zag structure with four spins per unit cell [15]. Magnetic moments are oriented orthogonally to honeycomb layers indicating the easy-axis anisotropy. The excitation spectrum consists of two double-degenerate magnon branches that were observed in the inelastic neutron scattering experiments [16–18]. Comparison with the neutron data allows us to assign the M_S and M_A modes to 1-magnon ($S_z = \pm 1$) excitations with $k = 0$ corresponding to in-phase and out-of-phase oscillations of parallel magnetic sublattices, respectively.

The low-energy mode M_S has been identified as the 1-magnon gap also in preceding optical (Raman scattering) studies [19]. In a magnetic field, this mode splits into two AFMR branches (1) separated by twice the Zeeman energy [20]. The corresponding g factor is $g_S \approx 2.15$ (Figure 2c). At higher magnetic fields, the lower branch of the M_S mode departs from a linear field dependence (Figures. 2b,c). This is due to a significant magnon-phonon coupling recently reported for FePS₃ [11, 21–23]. The solid line in Figure 2c that describes this coupling is a fit, using the model and its parameters discussed in Ref. 11 in detail. The upper 1-magnon gap M_A exhibits the same AFMR-like splitting, $g_A = g_S$, cf. Figures 2c and 2f. Interestingly, no traces of this upper 1-magnon

gap have so far been found in Raman scattering measurements to the best of our knowledge, nevertheless, its existence is clearly evidenced, *e.g.*, in neutron scattering experiments [17].

To develop a quantitative description of the observed resonance modes, we use the spin model for FePS₃ based on the neutron experiments [16, 17]. The spin Hamiltonian of FePS₃ includes the Heisenberg exchange interactions up to the third neighbours as well as the single-ion anisotropy and Zeeman terms:

$$\hat{\mathcal{H}} = J_1 \sum_{\langle ij \rangle} \mathbf{S}_i \cdot \mathbf{S}_j + J_2 \sum_{\langle ij \rangle} \mathbf{S}_i \cdot \mathbf{S}_j + J_3 \sum_{\langle ij \rangle} \mathbf{S}_i \cdot \mathbf{S}_j - D \sum_i (S_i^z)^2 + g\mu_B B \sum_i S_i^z. \quad (2)$$

The zigzag antiferromagnetic order observed in FePS₃ is stable for a sufficiently strong antiferromagnetic third-neighbour coupling $J_3 > 0$ [24]. Let us emphasize that this Hamiltonian is strictly two-dimensional, thus neglecting any inter-layer exchange coupling between spins. Such an approach is corroborated by results of neutron scattering measurements [17], but also Raman scattering experiments [25, 26] which indicate that FePS₃ keeps antiferromagnetic ordering down to the monolayer thickness, with the Néel temperature barely changed. Hence, bulk FePS₃ is a unique system that allows us to address, by means of optical tools, two-dimensional magnons – excitations seemingly untraceable in a monolayer sample (see Refs. 25 and 26).

The magneto-optical experiments probe uniform magnon modes with $k = 0$. For large- S antiferromagnets, the conventional single-magnon excitations can be obtained rather accurately by the harmonic spin-wave theory. Details of the corresponding calculations are presented in the Supplementary material [14]. The four uniform modes split into two pairs corresponding to the in-phase and out-of-phase oscillations of parallel sublattices in the up-up-down-down magnetic structure of FePS₃. The two symmetric modes have energies:

$$\Delta_S = 2S\sqrt{D(D + J_1 + 4J_2 + 3J_3)} \pm g\mu_B B, \quad (3)$$

whereas the antisymmetric modes are:

$$\Delta_A = 2S\sqrt{(D - 2J_1 + 4J_2)(D - J_1 + 3J_3)} \pm g\mu_B B. \quad (4)$$

In collinear antiferromagnetic structures with a rotation symmetry around the easy axis, magnons have a well-defined quantum numbers $S_z = \pm 1$. An applied magnetic field splits every degenerate pair of modes into descending and ascending branches with the bare g -factor, $g_{S,A} \approx 2.15$ in FePS₃. To get numerical estimates, we use the microscopic parameters obtained by Lancon *et al.* [17] from experimental fits of magnon bands (in meV):

$$J_1 = -2.92, \quad J_2 = 0.08, \quad J_3 = 1.92, \quad D = 2.66. \quad (5)$$

Because of a different convention used for presenting the lattice sums in the spin Hamiltonian (2), the above values for the exchange constants J_n differ by a factor of -2 from those given in Ref. 17. Using Eqs. (3) and (4) we reproduce the two lowest resonance modes measured in our experiments with an accuracy of 1–3 %.

Let us now consider the third mode M_4 which is observed at a high energy, $\Delta_4 = 57.5$ meV (at $B = 0$). Notably, this energy is slightly smaller than four times the energy of the lowest magnon: $\Delta_4 \lesssim 4\Delta_S \approx 60.4$ meV. Under magnetic field, the M_4 mode splits into two components with the effective g -factor $g_4 \approx 4g_{S,A}$. Such a relation points at a 4-magnon nature of this extra mode. The strong easy-axis anisotropy observed in FePS₃ can provide a mechanism for the creation of additional low-energy excitations besides the conventional magnon modes. Full reversal of a single spin, say, from $S_z = +S$ to $S_z = -S$ does not change the single-ion energy and costs only the energy of broken exchange bonds. It carries a high angular momentum $|S_z| = 2S$, which in the case of FePS₃ amounts to $|S_z| = 4$. The ordinary magnons have instead $|S_z| = 1$ irrespective of the spin quantum number of constituent magnetic ions. We shall use the term multipolar magnons for the full spin reversal excitations. The conventional magnons correspond in this terminology to dipolar excitations. A multipolar magnon can be viewed as $2S$ ordinary magnons attracted to the same lattice site by the single-ion anisotropy. Thus, this excitation can be alternatively named a single-ion bound state [13] in contrast to the exchange bound states discussed, for example, in Refs. 27–33.

The interest in single-ion bound states, sometimes also referred to as longitudinal magnons, has a long history. The focus of the majority of experimental [34–41] and theoretical [13, 42–45] studies was so far on $S = 1$ magnets. In spin-1 materials, 2-magnon bound states with $|S_z| = 2$ may appear and lead to quadrupolar or spin-nematic instabilities [43, 44]. More recently, the observations of bound states of more than two magnons have been reported. The 3-magnon bound state was found in α -NaMnO₂ ($S = 2$) using the neutron scattering technique [46], whereas the 4- and 6-magnon bound states hybridized with 1-magnon excitations were observed using the time-domain THz magneto-spectroscopy in FeI₂ ($S = 1$) [47]. Nevertheless, in both cases, the observed bound states are composed of bound magnons located on adjacent lattice sites, and therefore, correspond to the exchange bound states. Note that the multi-magnon bound states are to be distinguished from other excitations involving multiple 1-magnon states reported experimentally, see, *e.g.*, Refs. 48–50.

To corroborate our interpretation, let us estimate the energy of the M_4 mode. In the crudest approximation, we neglect dispersion of a multipolar magnon and compute its energy by inverting fully one spin in the zigzag antiferromagnetic structure of FePS₃ [14]:

$$\Delta_4 = 2S^2(3J_3 - J_1 + 2J_2) \pm 4g\mu_B B. \quad (6)$$

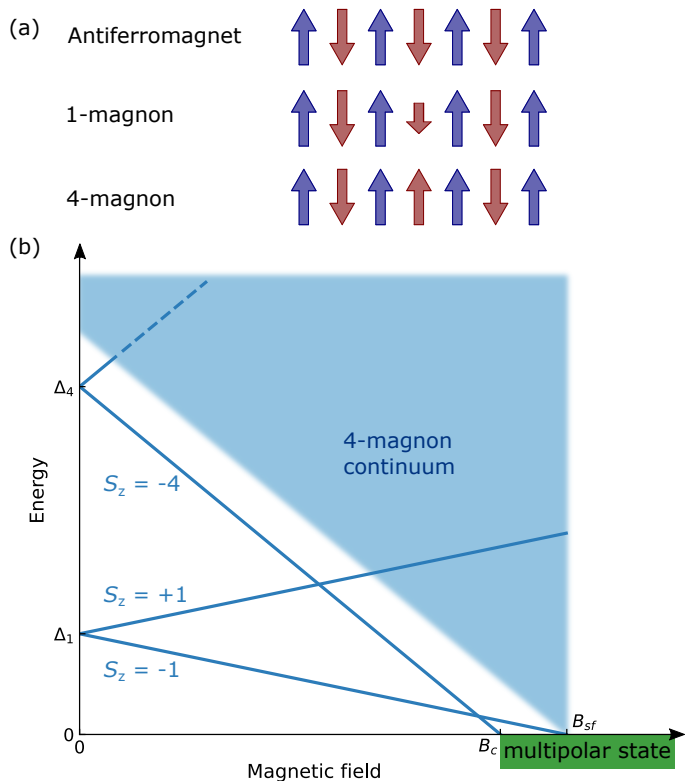


FIG. 3. Exotic excitations and states in a collinear $S = 2$ antiferromagnet. Panel (a): Schematic representation of a 1-magnon excitation and a 4-magnon excitation. Panel (b): Resonance $k = 0$ modes in a magnetic field applied along the easy axis. Δ_1 and Δ_4 denote the AFMR and the 4-magnon gaps, respectively. The condensation of the AFMR mode results in the usual spin flop transition at $B = B_{sf}$, whereas condensation of a 4-magnon at $B = B_c$ signifies appearance of a multipolar state.

The two branches, degenerate at $B = 0$, correspond to spin flips on up and down sublattices. The relation $g_4 = 4g$ remains exact for the continuous spin-rotation symmetry about the z axis present in the spin Hamiltonian (2). A small deviation observed experimentally $g_4/g \approx 4.3$ can be attributed to weak spin-orbit effects. Notably, the above expressed 4-magnon energy – corresponding to a full spin inversion – does not depend on the D parameter. This is because the magnetic anisotropy term in Hamiltonian (2) is even in S_z . In contrast, the energies of 1-magnon excitations (3,4), and consequently, also various bound states of 1-magnons located on different lattice sites, always scale with D .

Using Eq. (6) and the microscopic parameters (5), we obtain $\Delta_4^{\text{th}} = 71$ meV, which slightly deviates from the experimental value $\Delta_4 = 57.5$ meV. One of the effects not included in the theoretical expression (6) is the dispersion of the multipolar magnon. This problem can be approached in the strong-coupling limit $D \gg |J_n|$. For $S = 2$, the transverse coupling of full spin flips on adjacent sites appears only in the fourth-order of the perturbative expansion $\mathcal{J}_\perp \simeq J_n^4/(8D^3)$ in comparison to the

second-order effect for $S = 1$ [43, 44]. Since in FePS₃ $D \sim |J_1|$, a more elaborated theoretical treatment is necessary to calculate the dispersion of a single-ion 4-magnon bound state.

Nevertheless, the principal source of the discrepancy is likely related to the presence of a significant biquadratic exchange in FePS₃ as recently argued by Wildes *et al.* [18] from a detailed fit of the early inelastic neutron-scattering results. Obviously, such additional terms do not affect the multipolar magnon energy computed in the ‘Ising’ approximation (6), whereas they affect the 1-magnon dispersion, modifying an appropriate choice of the bilinear exchanges. Taking instead of (5) the exchange constants $J_1 = -2.92$ meV, $J_2 = 0.44$ meV and $J_3 = 1.1$ meV reported in Ref. 18, we obtain $\Delta_4^{\text{th}} = 56.8$ meV in a perfect match with our experimental value.

Because of their high-angular momentum, the multipolar magnons should not be nominally seen using experimental probes that obey the dipolar selection rules. This corresponds to both the magneto-optical measurements and the neutron-scattering experiments. Our observation of such excitations is related to the fact that FePS₃ has weak additional spin-orbit terms not included in Eq. 2 that break continuous rotation symmetry about the z direction. When interlayer coupling is neglected, we deal with a trigonal symmetry in FePS₃. As a result, there is a weak hybridization between $S_z = 4$ and $S_z = 1$ excitations [14], which enables observation of multipolar magnons. Hence, even though the strength of the spin-orbit interaction – quantified by the magnetic anisotropy D – does not directly enter the energy of the observed 4-magnon single-ion bound state (6), its role is still very important. First, it is responsible for a relatively high energy of the lower 1-magnon gap, and consequently, also for the high onset of the 4-magnon continuum ($4\Delta_S$). This results in a relatively broad spectral window, in which the 4-magnon single-ion bound states can be searched. Second, it couples the local spin to the surrounding (orbital) crystal field thanks to which a multipolar magnon state can become optically active. Third, it stabilizes the 4-magnon single-ion bound state.

We finish with a brief comment on possible new magnetic-field-induced states related to the presence of multipolar magnons. For an easy-axis antiferromagnet with a moderate anisotropy $D \sim J$ and an arbitrary spin $S \geq 1$, a multipolar magnon may split down from the $2S$ -magnon continuum. The schematic frequency-field diagram is illustrated in Figure 3 for a specific spin value $S = 2$. The multipolar magnon will condense [51] in a magnetic field of $g_4\mu_B B_c = \Delta_4$ before a conventional

spin-flop transition appears at $g\mu_B B_{\text{sf}} = \Delta_1$. The nature of the high-field phase emerging at $B > B_c$ depends on the angular momentum of the condensed excitation. For $S = 1$, this state breaks the quadrupolar symmetry and corresponds to a spin nematic phase [43, 44]. For larger spins $S > 1$, higher-order multipoles are necessary for description of the symmetry-broken state. In particular, for $S = 3/2$ and $S = 2$, the corresponding order parameters have octupole and hexadecapole symmetry, respectively. Further details, for example, the instability wavevector at $B = B_c$, depend on the dispersion of multipolar magnons, which represents an interesting theoretical problem for future studies. Thus, contrary to conventional wisdom, which suggests a semiclassical behavior for magnets with $S > 1$, the unconventional states arising from the condensation of multipolar magnons promise to be very interesting and exotic.

In conclusion, we have explored the magneto-optical response of the quasi-two-dimensional antiferromagnetic semiconductor FePS₃ and we have identified a novel magnetic excitation. It closely resembles the conventional AFMR, typical of easy-axis antiferromagnets, nevertheless, with a splitting four times larger than expected for 1-magnon gaps. We argue that we observe a multipolar excitation (single-ion 4-magnon bound state) which corresponds to a full reversal of a single Fe²⁺ iron spin and carries a total angular momentum of $|S_z| = 4$. This opens a venue for exotic hexadecapole phases.

ACKNOWLEDGMENTS

We acknowledge useful discussions with Andrew Wildes. The work has been supported by the EU Graphene Flagship project. M.V. acknowledges the support by the Operational Program Research, Development and Education financed by European Structural and Investment Funds and the Czech Ministry of Education, Youth and Sports (Project MATFUN – CZ.02.1.01/0.0/0.0/15_003/0000487). M.E.Z. acknowledges support by the ANR, France, Grant No. ANR-19-CE30-0004. The work was supported by the Czech Science Foundation, project No. 22-21974S and by the Czech-French exchange programme PHC BARRANDE (48101TB). This research was supported by the NCCR MARVEL, a National Centre of Competence in Research, funded by the Swiss National Science Foundation (grant number 205602).

-
- [1] C. Kittel, On the theory of ferromagnetic resonance absorption, *Phys. Rev.* **73**, 155 (1948).
 [2] C. Kittel, Theory of antiferromagnetic resonance, *Phys. Rev.* **82**, 565 (1951).
 [3] K. Momma and F. Izumi, Vesta3 for three-dimensional

- visualization of crystal, volumetric and morphology data, *Journal of Applied Crystallography* **44**, 1272 (2011).
 [4] F. Keffer and C. Kittel, Theory of antiferromagnetic resonance, *Phys. Rev.* **85**, 329 (1952).
 [5] D. Petitgrand and P. Meyer, Far infrared antiferromag-

- netic resonance in FeCl_2 , FeBr_2 and FeI_2 , *Journal de Physique* **37**, 1417 (1976).
- [6] M. Hagiwara, K. Katsumata, H. Yamaguchi, M. Tokunaga, I. Yamada, M. Gross, and P. Goy, A complete frequency-field chart for the antiferromagnetic resonance in MnF_2 , *J. Infrared Millim. Waves* **20**, 617 (1999).
- [7] P. R. Elliston and G. J. Troup, Some antiferromagnetic resonance measurements in $\alpha\text{-Fe}_2\text{O}_3$, *J. Phys. C: Solid State Phys.* **1**, 169 (1968).
- [8] D. Fowles and C. Stager, Antiferromagnetic resonance in $\text{Mn}_2\text{P}_2\text{O}_7$, *Can. J. Phys.* **50**, 2681 (1972).
- [9] L. Mihály, D. Talbayev, L. F. Kiss, J. Zhou, T. Fehér, and A. Jánosy, Field-frequency mapping of the electron spin resonance in the paramagnetic and antiferromagnetic states of LaMnO_3 , *Phys. Rev. B* **69**, 024414 (2004).
- [10] J. Zhang, M. Bialek, A. Magrez, H. Yu, and J.-P. Ansermet, Antiferromagnetic resonance in TmFeO_3 at high temperatures, *J. Magn. Magn. Mater.* **523**, 167562 (2021).
- [11] D. Vaclavkova, M. Palit, J. Wyzula, S. Ghosh, A. Delhomme, S. Maity, P. Kapuscinski, A. Ghosh, M. Veis, M. Grzeszczyk, C. Faugeras, M. Orlita, S. Datta, and M. Potemski, Magnon polarons in the van der Waals antiferromagnet FePS_3 , *Phys. Rev. B* **104**, 134437 (2021).
- [12] J.-G. Park, Opportunities and challenges of 2d magnetic van der waals materials: magnetic graphene?, *J. Phys.: Condens. Matter* **28**, 301001 (2016).
- [13] R. Silberglitt and J. B. Torrance, Effect of single-ion anisotropy on two-spin-wave bound state in a Heisenberg ferromagnet, *Phys. Rev. B* **2**, 772 (1970).
- [14] See Supplementary material for details of theoretical calculations and discussion about additional weak AFMR-like features.
- [15] K. C. Rule, G. J. McIntyre, S. J. Kennedy, and T. J. Hicks, Single-crystal and powder neutron diffraction experiments on FePS_3 : Search for the magnetic structure, *Phys. Rev. B* **76**, 134402 (2007).
- [16] A. R. Wildes, K. C. Rule, R. I. Bewley, M. Enderle, and T. J. Hicks, The magnon dynamics and spin exchange parameters of FePS_3 , *J. Phys.: Condens. Matter* **24**, 416004 (2012).
- [17] D. Lançon, H. C. Walker, E. Ressouche, B. Oulad-diaf, K. C. Rule, G. J. McIntyre, T. J. Hicks, H. M. Rønnow, and A. R. Wildes, Magnetic structure and magnon dynamics of the quasi-two-dimensional antiferromagnet FePS_3 , *Phys. Rev. B* **94**, 214407 (2016).
- [18] A. R. Wildes, M. E. Zhitomirsky, T. Ziman, D. Lançon, and H. C. Walker, Evidence for biquadratic exchange in the quasi-two-dimensional antiferromagnet FePS_3 , *J. Appl. Phys.* **127**, 223903 (2020).
- [19] T. Sekine, M. Jouanne, C. Julien, and M. Balkanski, Light-scattering study of dynamical behavior of antiferromagnetic spins in the layered magnetic semiconductor FePS_3 , *Phys. Rev. B* **42**, 8382 (1990).
- [20] A. McCreary, J. R. Simpson, T. T. Mai, R. D. McMichael, J. E. Douglas, N. Butch, C. Dennis, R. Valdés Aguilar, and A. R. Hight Walker, Quasi-two-dimensional magnon identification in antiferromagnetic FePS_3 via magneto-Raman spectroscopy, *Phys. Rev. B* **101**, 064416 (2020).
- [21] S. Liu, A. Granados del Águila, D. Bhowmick, C. K. Gan, T. Thu Ha Do, M. A. Prosnikov, D. Sedmidubský, Z. Sofer, P. C. M. Christianen, P. Sengupta, and Q. Xiong, Direct observation of magnon-phonon strong coupling in two-dimensional antiferromagnet at high magnetic fields, *Phys. Rev. Lett.* **127**, 097401 (2021).
- [22] Q. Zhang, M. Ozerov, E. V. Boström, J. Cui, N. Suri, Q. Jiang, C. Wang, F. Wu, K. Hwangbo, J.-H. Chu, *et al.*, Coherent strong-coupling of terahertz magnons and phonons in a Van der Waals antiferromagnetic insulator, preprint, arXiv:2108.11619 [10.48550/arXiv.2108.11619](https://arxiv.org/abs/2108.11619) (2021).
- [23] A. Pawbake, T. Pelini, A. Delhomme, D. Romanin, D. Vaclavkova, G. Martinez, M. Calandra, M.-A. Measson, M. Veis, M. Potemski, M. Orlita, and C. Faugeras, High-pressure tuning of magnon-polarons in the layered antiferromagnet FePS_3 , *ACS Nano* **16**, 12656 (2022).
- [24] J. B. Fouet, P. Sindzingre, and C. Lhuillier, An investigation of the quantum J_1 - J_2 - J_3 model on the honeycomb lattice, *Eur. Phys. J. B* **20**, 241 (2001).
- [25] J.-U. Lee, S. Lee, J. H. Ryoo, S. Kang, T. Y. Kim, P. Kim, C.-H. Park, J.-G. Park, and H. Cheong, Ising-type magnetic ordering in atomically thin FePS_3 , *Nano Letters* **16**, 7433 (2016).
- [26] X. Wang, K. Du, Y. Y. F. Liu, P. Hu, J. Zhang, Q. Zhang, M. H. S. Owen, X. Lu, C. K. Gan, P. Sengupta, *et al.*, Raman spectroscopy of atomically thin two-dimensional magnetic iron phosphorus trisulfide (feps_3) crystals, *2D Materials* **3**, 031009 (2016).
- [27] M. Wortis, Bound states of two spin waves in the Heisenberg ferromagnet, *Phys. Rev.* **132**, 85 (1963).
- [28] J. Hanus, Bound states in the Heisenberg ferromagnet, *Phys. Rev. Lett.* **11**, 336 (1963).
- [29] T. Oguchi and T. Ishikawa, Theory of two-magnon bound states in a two-dimensional antiferromagnet, *J. Phys. Soc. Jpn.* **34**, 1486 (1973).
- [30] A. V. Chubukov, Chiral, nematic, and dimer states in quantum spin chains, *Phys. Rev. B* **44**, 4693(R) (1991).
- [31] N. Shannon, T. Momoi, and P. Sindzingre, Nematic order in square lattice frustrated ferromagnets, *Phys. Rev. Lett.* **96**, 027213 (2006).
- [32] C. J. Hamer, Energy spectrum of the two-magnon bound states in the Heisenberg-Ising antiferromagnet on the square lattice, *Phys. Rev. B* **79**, 212413 (2009).
- [33] M. E. Zhitomirsky and H. Tsunetsugu, Magnon pairing in quantum spin nematic, *EPL* **92**, 37001 (2010).
- [34] A. Fert, D. Bertrand, J. Leotin, J. Ousset, J. Magarino, and J. Tuchendler, Excitation of two spin deviations by far infrared absorption in FeI_2 , *Solid State Commun.* **26**, 693 (1978).
- [35] A. A. Baharmuz and P. D. Loly, Two-magnon excitations in the Heisenberg ferromagnet with uniaxial anisotropy, *Phys. Rev. B* **22**, 1294 (1980).
- [36] D. Petitgrand, A. Brun, and P. Meyer, Magnetic field dependence of spin waves and two magnon bound states in FeI_2 , *J. Magn. Magn. Mater.* **15-18**, 381 (1980).
- [37] G. C. Psaltakis, G. Mischler, D. J. Lockwood, M. G. Cottam, A. Zwick, and S. Legrand, One- and two-magnon excitations in FeBr_2 , *J. Phys. C: Solid State Phys.* **17**, 1735 (1984).
- [38] M. Orendáč, S. Zvyagin, A. Orendáčová, M. Sieling, B. Lüthi, A. Feher, and M. W. Meisel, Single-ion bound states in $S = 1$ Heisenberg antiferromagnetic chains with planar anisotropy and subcritical exchange coupling, *Phys. Rev. B* **60**, 4170 (1999).
- [39] S. A. Zvyagin, J. Wosnitza, C. D. Batista, M. Tsukamoto, N. Kawashima, J. Krzystek, V. S. Zapf, M. Jaime,

- N. F. Oliveira, and A. Paduan-Filho, Magnetic excitations in the spin-1 anisotropic Heisenberg antiferromagnetic chain system $\text{NiCl}_2\text{-4SC}(\text{NH}_2)_2$, *Phys. Rev. Lett.* **98**, 047205 (2007).
- [40] S. Zvyagin, C. Batista, J. Krzystek, V. Zapf, M. Jaime, A. Paduan-Filho, and J. Wosnitza, Observation of two-magnon bound states in the spin-1 anisotropic Heisenberg antiferromagnetic chain system $\text{NiCl}_2\text{-4SC}(\text{NH}_2)_2$, *Phys. B: Condens. Matter* **403**, 1497 (2008).
- [41] X. Bai, S.-S. Zhang, Z. Dun, H. Zhang, Q. Huang, H. Zhou, M. B. Stone, A. I. Kolesnikov, F. Ye, C. D. Batista, and M. Mourigal, Hybridized quadrupolar excitations in the spin-anisotropic frustrated magnet FeI_2 , *Nature Phys.* **17**, 467 (2021).
- [42] N. Papanicolaou and G. C. Psaltakis, Bethe ansatz for two-magnon bound states in anisotropic magnetic chains of arbitrary spin, *Phys. Rev. B* **35**, 342 (1987).
- [43] K. Damle and T. Senthil, Spin nematics and magnetization plateau transition in anisotropic kagome magnets, *Phys. Rev. Lett.* **97**, 067202 (2006).
- [44] K. Wierschem, Y. Kato, Y. Nishida, C. D. Batista, and P. Sengupta, Magnetic and nematic orderings in spin-1 antiferromagnets with single-ion anisotropy, *Phys. Rev. B* **86**, 201108 (2012).
- [45] A. V. Sizanov and A. V. Syromyatnikov, Spin nematic states in spin-1 antiferromagnets with easy-axis anisotropy, *JETP Lett.* **97**, 107 (2013).
- [46] R. L. Dally, A. J. R. Heng, A. Keselman, M. M. Bordelon, M. B. Stone, L. Balents, and S. D. Wilson, Three-magnon bound state in the quasi-one-dimensional antiferromagnet $\alpha\text{-NaMnO}_2$, *Phys. Rev. Lett.* **124**, 197203 (2020).
- [47] A. Legros, S.-S. Zhang, X. Bai, H. Zhang, Z. Dun, W. A. Phelan, C. D. Batista, M. Mourigal, and N. P. Armitage, Observation of 4- and 6-magnon bound states in the spin-anisotropic frustrated antiferromagnet FeI_2 , *Phys. Rev. Lett.* **127**, 267201 (2021).
- [48] R. E. Dietz, W. F. Brinkman, A. E. Meixner, and H. J. Guggenheim, Raman scattering by four magnons in NiO and KNiF_3 , *Phys. Rev. Lett.* **27**, 814 (1971).
- [49] M. G. Cottam, Theory of two-magnon Raman scattering in antiferromagnets at finite temperatures, *J. Phys. C: Solid State Phys.* **5**, 1461 (1972).
- [50] E. Funkenbusch and B. Cornilsen, Two-magnon Raman scattering in calcium doped NiO , *Solid State Commun.* **40**, 707 (1981).
- [51] V. Zapf, M. Jaime, and C. D. Batista, Bose-Einstein condensation in quantum magnets, *Rev. Mod. Phys.* **86**, 563 (2014).

Supplementary Information for:
High-angular momentum excitations in collinear antiferromagnet FePS₃

Jan Wyzula,^{1,2} Ivan Mohelský,¹ Diana Václavková,¹ Piotr Kapuscinski,¹ Martin Veis,³
 Clément Faugeras,¹ Marek Potemski,^{1,4} Mike E. Zhitomirsky,⁵ and Milan Orlita^{1,3}

¹*Laboratoire National des Champs Magnétiques Intenses, EMFL,*

CNRS UPR3228, Univ. Grenoble Alpes, Univ. Toulouse,

Univ. Toulouse 3, INSA-T, Grenoble and Toulouse, F-38042, France

²*Department of Physics, University of Fribourg, Chemin du Musée 3, CH-1700 Fribourg, Switzerland*

³*Institute of Physics, Charles University, Ke Karlovu 5, Prague, CZ-121 16, Czech Republic*

⁴*CENTERA Labs, Institute of High Pressure Physics, PAS, PL-01-142 Warsaw, Poland*

⁵*Univ. Grenoble Alpes, CEA, IRIG, PHELIQS,*
17 avenue des Martyrs, F-38000 Grenoble, France

(Dated: November 22, 2022)

Spin Hamiltonian and AFMR modes

Here we briefly outline basic steps and main results of the spin-wave calculations for the AFMR spectrum of the zig-zag antiferromagnetic state on a honeycomb lattice realized by iron moments in FePS₃. The geometry of the exchange couplings and the resulting zig-zag antiferromagnetic structure are schematically shown in Fig. S1. The magnetic unit cell contains two \uparrow and two \downarrow pointing sublattices that are indexed as shown in Fig. S1.

The microscopic spin Hamiltonian of FePS₃ includes Heisenberg exchange interactions and the single-ion anisotropy:

$$\hat{\mathcal{H}} = \sum_{\langle ij \rangle} J_{ij} \mathbf{S}_i \cdot \mathbf{S}_j - D \sum_i (S_i^z)^2 + g\mu_B B \sum_i S_i^z, \quad (\text{S1})$$

where J_{ij} extend up to the third-neighbor shell. Note that due to a different convention used in writing the spin-pair sums, we need to multiply by a factor of -2 the exchange constants deduced by Lancon et al. [1].

The AFMR modes correspond to $k = 0$ excitations. Therefore, instead of studying the full lattice Hamiltonian (S1), we can project it to the four sublattice state:

$$\begin{aligned} \hat{\mathcal{H}} = & J_1 [2\mathbf{S}_1 \cdot \mathbf{S}_2 + 2\mathbf{S}_3 \cdot \mathbf{S}_4 + \mathbf{S}_1 \cdot \mathbf{S}_3 + \mathbf{S}_2 \cdot \mathbf{S}_4] + 4J_2 (\mathbf{S}_1 \cdot \mathbf{S}_4 + \mathbf{S}_2 \cdot \mathbf{S}_3) \\ & + 3J_3 (\mathbf{S}_1 \cdot \mathbf{S}_3 + \mathbf{S}_2 \cdot \mathbf{S}_4) - D(S_{1z}^2 + S_{2z}^2 + S_{3z}^2 + S_{4z}^2) + g\mu_B B (S_{1z} + S_{2z} + S_{3z} + S_{4z}). \end{aligned} \quad (\text{S2})$$

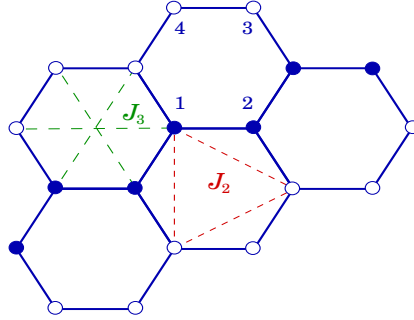


FIG. S1: J_1 - J_2 - J_3 Heisenberg spin model on a honeycomb lattice. Full and empty circles represent up and down spins in the zig-zag antiferromagnetic structure of FePS₃.

We now apply the Holstein-Primakoff transformation for the spin operators and obtain in a quadratic order:

$$\begin{aligned} \hat{\mathcal{H}}_2 = & S(2D + 3J_3 - J_1 + 4J_2)(a_1^\dagger a_1 + a_2^\dagger a_2 + a_3^\dagger a_3 + a_4^\dagger a_4) + g\mu_B B (a_1^\dagger a_1 + a_2^\dagger a_2 - a_3^\dagger a_3 - a_4^\dagger a_4) + \\ & + 2J_1 S (a_1^\dagger a_2 + a_2^\dagger a_1 + a_3^\dagger a_4 + a_4^\dagger a_3) - (3J_3 + J_1)(a_1 a_3 + a_2 a_4 + a_3^\dagger a_1^\dagger + a_4^\dagger a_2^\dagger) \\ & - 4J_2 S (a_1 a_4 + a_2 a_3 + a_4^\dagger a_1^\dagger + a_3^\dagger a_2^\dagger). \end{aligned} \quad (\text{S3})$$

Performing standard steps of diagonalization of such Hamiltonians: (i) introducing symmetric/asymmetric bosons for (1,2) and (3,4) spin pairs and (ii) canonical Bogolyubov transformation we obtain two pairs of AFMR modes. The low-energy symmetric excitations have energy gaps:

$$\Delta_S = 2S\sqrt{D(D + J_1 + 3J_3 + 4J_2)} \pm g\mu_B B, \quad (\text{S4})$$

whereas the higher-lying antisymmetric modes are given as:

$$\Delta_A = 2S\sqrt{(D - 2J_1 + 4J_2)(D + 3J_3 - J_1)} \pm g\mu_B B. \quad (\text{S5})$$

The \pm signs in the above expression signify that both lower and upper pairs of excitations consist of magnons with $S_z = \pm 1$.

Let us now compute the energy of a fully reversed spin neglecting, at the same time, its dispersion. The energy costs of such an excitation is obtained by counting broken bonds:

$$\Delta_4 = S^2(-2J_1 + 6J_3 + 4J_2) \pm 4g\mu_B B, \quad (\text{S6})$$

from which we obtain the expression given in the main text.

Additional observed AFMR-like modes

Besides the resonance modes M_S , M_A and M_4 discussed in detail in the main text, we have also identified additional AFMR-like spectral features in our data. These include the M_α and M_β modes observed nearby the M_4 mode and another AFMR-like excitation at lower photon energies denoted as M_2 . These three additional modes are clearly visible in Fig. S2. Notably, their integral intensities are significantly weaker – approximately by a factor of 10^{-3} for the M_2 excitation and by a factor of 10^{-4} for the M_α and M_β modes – as compared to the 1-magnon gaps M_S and M_A . The effective g factors extracted from slopes, $g_2 = (4.2 \pm 0.2)$, $g_\alpha = (7.3 \pm 0.5)$ and $g_\beta = (5.0 \pm 0.5)$, provide us with a clear indication of their multi-magnon/multipolar nature. We attribute their appearance in FePS₃ to the balance between strong easy-axis anisotropy D and nearest-neighbour ferromagnetic exchange interaction J_1 .

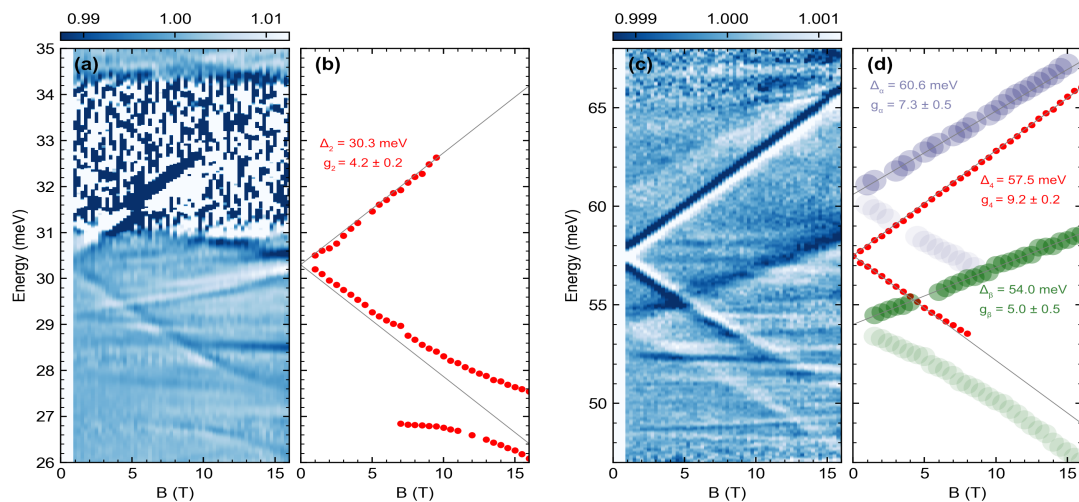


FIG. S2: False-color maps of differential magneto-transmission measured on FePS₃ ($T_B/T_{B-\Delta B}$ for $\Delta B = 1$ T, with a step 0.25 T) in two spectral windows in panels (a) and (c). The extracted positions of resonances at selected values of B are plotted in panels (b) and (d), respectively. The size and transparency of the full circles in (d) are chosen to approximately match the error bar and the strength of transitions. The position of resonance at $B = 0$ and the effective g factor were obtained via a fit, using the standard AFMR formula: $\omega_{\text{AFMR}} = \Delta \pm g\mu_B B$. For the weaker M_α and M_β resonances, only the upper, significantly more pronounced branch was fitted. One may also observe that the lower branch of the M_β mode exhibits slightly non-linear in B evolution.

The M_2 mode, characterized by $g_2 = 4.2$ and by the energy of $\Delta_2 = 30.3$ meV, see Fig. S2a,b, corresponds to a quadrupolar excitation of two magnons from the bottom of the 1-magnon band ($\Delta_S = 15.1$ meV). Each magnon in such a pair corresponds to a propagating plane wave. They seem to interact, independently of each other, with an optical phonon mode at 13.5 meV. This gives rise to avoided crossing behavior that is observed for the lower branch of the M_2 excitation around the photon energy of 27 meV. Such a coupling is consistent with magnon-phonon interaction observed recently for the lower 1-magnon gap in FePS₃ [2, 3]. The pair of magnons can reduce their energy by enhancing a probability for states with two spin flips occupying nearby lattice sites. The binding energy then may shift the 2-magnon excitation below the 2-magnon continuum at $2\Delta_S$. Nevertheless, in this particular case, we find $\Delta_2 \approx 2\Delta_S$ and the binding energy thus seems to be negligible.

The M_α mode, with $g_\alpha = 7.3$ and $\Delta_\alpha = 60.6$ meV, may correspond to a bound complex of three 1-magnon excitations, thus having the octupolar symmetry. The AFMR-like mode M_β at $\Delta_\beta = 54.0$ meV exhibits a bit lower effective g factor, $g_\beta = 5.0$, as compared to the M_α mode which may point towards its 2-magnon character. Since the energy Δ_β exceeds the onset of the 2-magnon continuum for the lower 1-magnon gap (*i.e.*, twice Δ_S), it is plausible to assume that the M_β mode is a bound state of two magnons from the upper 1-magnon gap. Note that all these modes can further hybridize with conventional 1-magnons and 4-magnon single-ion bound states due to spin-orbit coupling. Widely varying absorption intensities of different resonance modes are determined by matrix elements, which couple the ground state with a given multipolar excitation. Abundance of distinct resonance modes in FePS₃ – presented here, but likely also yet to be discovered – makes it an interesting model system for studying nontrivial quantum excitations in almost semiclassical ($S = 2$) magnetic materials.

Let us add that, following the lower branch of the M_4 excitation as a function of B , we may see that its visibility in the spectra, see Fig. S2c, decreases when it enters the spectral range of 51-54 meV. In this range, we observe weakly B -dependent, *i.e.*, nearly horizontal in Fig. S2h, spectral features. We interpret them as multi-phonon resonances which become B -dependent due to magnon-phonon coupling (clearly present in FePS₃ and studied experimentally see Refs. [2, 3]) and which may effectively broaden/mask the lower branch of the 4-magnon excitation.

-
- [1] D. Lancon, H. C. Walker, E. Ressouche, B. Ouladdiaf, K. C. Rule, G. J. McIntyre, T. J. Hicks, H. M. Ronnow, and A. R. Wildes, Phys. Rev. B **94**, 214407 (2016).
 - [2] Sheng Liu, Andras Granados del Aguila, Dhiman Bhowmick, Chee Kwan Gan, T. Thu Ha Do, M. A. Prosnikov, David Sedmidubsky, Zdenek Sofer, Peter C. M. Christianen, Pinaki Sengupta, and Qihua Xiong, Phys. Rev. Lett. **127**, 097401 (2021).
 - [3] D. Vaclavkova, M. Palit, J. Wyzula, S. Ghosh, A. Delhomme, S. Maity, P. Kapuscinski, A. Ghosh, M. Veis, M. Grzeszczyk, C. Faugeras, M. Orlita, S. Datta, and M. Potemski, Phys. Rev. B **104**, 134437 (2021).